Systematic transcriptome analysis allows the identification of new type I and type II Toxin/Antitoxin systems located in the superintegron of Vibrio cholerae

Evelyne Krin, Zeynep Baharoglu, Odile Sismeiro, Hugo Varet, Jean-Yves Coppée, Didier Mazel

HAL Id: pasteur-03889562
https://pasteur.hal.science/pasteur-03889562

Submitted on 8 Dec 2022

Original Article

Systematic transcriptome analysis allows the identification of new type I and type II Toxin/Antitoxin systems located in the superintegron of *Vibrio cholerae*

Evelyne Krin [a], Zeynep Baharoglu [a], Odile Sismeiro [b], Hugo Varet [b], Jean-Yves Coppée [b], Didier Mazel [a, *]

[a] *Institut Pasteur, Université Paris Cité, CNRS UMR 3525, Unité de Plasticité du Génome Bactérien, 28 rue du Docteur Roux, F-75015 Paris, France*
[b] *Institut Pasteur, Université Paris Cité, Transcriptome and EpiGenome, Biomics Center for Innovation and Technological Research, 28 rue du Docteur Roux, F-75015 Paris, France*

ARTICLE INFO

ABSTRACT

Vibrio cholerae N16961 genome encodes 18 type II Toxin/Antitoxin (TA) systems, all but one located inside gene cassettes of its chromosomal superintegron (SI). This study aims to investigate additional TA systems in this genome. We screened for all two-genes operons of uncharacterized function by analyzing previous RNAseq data. Assays on nine candidates, revealed one additional functional type II TA encoded by the VCA0497-0498 operon, carried inside a SI cassette. We showed that VCA0498 antitoxin alone and in complex with VCA0497 represses its own operon promoter. VCA0497-0498 is the second element of the recently identified *dhiT/dhiA* superfamily uncharacterized type II TA system. RNAseq analysis revealed that another SI cassette encodes a novel type I TA system: VCA0495 gene and its two associated antisense non-coding RNAs, ncRNA495 and ncRNA496. Silencing of both antisense ncRNAs lead to cell death, demonstrating the type I TA function. Both VCA0497 and VCA0495 toxins do not show any homology to functionally characterized toxins, however our preliminary data suggest that their activity may end up in mRNA degradation, directly or indirectly. Our findings increase the TA systems number carried in this SI to 19, preferentially located in its distal end, confirming their importance in this large cassette array.

© 2022 The Authors. Published by Elsevier Masson SAS on behalf of Institut Pasteur. This is an open access article under the CC BY license (http://creativecommons.org/licenses/by/4.0/).

1. Introduction

Vibrio cholerae is the cholera-causing bacterium, which leads to severe watery diarrhea and dehydration, often fatal for immuno-compromised individuals. Its genome is organized in two chromosomes: a large one (2.9 megabases) that contains most of the essential genes and a small one (1.0 megabases) [1], that carries a sedentary chromosomal integron gathering tens of gene cassettes, called a superintegron (SI) [2]. The SI platform consists of the integron integrase gene controlled by the SOS response and a strong promoter, Pc, allowing the expression of the first of the 176 cassettes long array [3,4] as approximately 75% of cassettes are promoterless, in the case of N16961 strain [5]. Cassettes carry genes of unknown functions or predicted to be of various adaptive functions (acetyltransferases, DNA modifying enzymes, restriction-modification enzymes, dNTP pyrophosphohydrolases, lipoproteins, metabolite binding proteins, glyoxalases, lipases, antibiotic resistance and virulence factors [6–9]). In addition, these arrays have been found to host a large number of cassettes encoding type II Toxin/Antitoxin (TA) systems, which have been shown to play a role for the stabilization of these large cassette arrays and are all carrying their own promoter [5,10–13].

Seven types of Toxin/Antitoxin (TA) systems have already been characterized in bacteria. They all consist of a toxin protein and an antitoxin that counteracts the toxin's action, either by inhibition, or by blocking its synthesis. According to the type of TA system, the antitoxin can be a protein (type II, IV to VII) or a non-coding RNA (ncRNA) (type I, III) [14,15]. Although there is a type III TA system in *V. cholerae* 0395 strain [16], only type II TA systems have been identified so far [10–12,17] in *V. cholerae* N16961 strain, isolated

* Corresponding author.
E-mail addresses: ekrin@pasteur.fr (E. Krin), zeynep.baharoglu@pasteur.fr (Z. Baharoglu), odile.sismeiro@pasteur.fr (O. Sismeiro), hugo.varet@pasteur.fr (H. Varet), jean-yves.coppee@pasteur.fr (J.-Y. Coppée), mazel@pasteur.fr (D. Mazel).

during the 7th pandemic. Type II TA system are organized in two-genes operons: one encodes a stable toxin that targets an essential cellular function (e.g. replication, translation, cell wall synthesis …) while the other encodes a labile antitoxin that inhibits the toxin. The differential stability of the two elements governs the preservation of the operon; indeed, upon loss of this operon, the rapid degradation of the antitoxin releases enough functional toxin to trigger cell death [18]. In addition to manage toxin inhibition by protein−protein binding, the antitoxin also often acts as a transcriptional autorepressor of the operon, alone or, usually, associated with the toxin (for reviews see [19]). In *V. cholerae*, all of the 18 Type II TA systems, except one, are located inside the SI cassette array [12] and carry their own promoter [5]. They are proposed to stabilize the SI by minimizing genomic reduction and loss of gene cassettes, due to the lack of selective advantage of silent cassettes in the absence of stress triggering cassette shuffling [10−13,17]. Type I TA systems are more difficult to identify than type II TA. Indeed, type I TA systems are generally composed of a gene encoding an hydrophobic toxic protein and a small antisense (AS) RNA, that plays the antitoxin role, by repressing the toxin synthesis through base pairing with the toxin mRNA, such as in the *tisB/itsR1* and *hok-sok* systems [20,21]. Nevertheless, bioinformatics analyses based on characteristics of known loci (e.g. clusters of charged and bulky amino acids, short proteins, transmembrane regions), allowed Fozo and collaborators to identify new type I TA systems in *Escherichia coli* and *Bacillus subtilis* [22].

In the present work, RNAseq data were used to search for and discover new TA systems. We first used our published RNAseq and TSS data [5] to identify potential TA system by screening for 2-genes long operons. This led to the discovery and characterization of a new type II TA system, which is carried in an integron cassette, like most type II TA system of *V. cholerae*. Moreover, since we had previously mapped all ncRNAs of N16961 strain [5], we systematically analyzed ncRNA presence inside the SI cassettes which carry a gene possessing its own promoter. This analysis allowed the identification of a new type I TA system candidate. In vivo assays were then performed to characterize their functionality.

2. Materials and methods

2.1. Bacterial strains, plasmids and growth conditions

The bacterial strains are listed in Supplementary Table S2. Plasmids are listed in Supplementary Table S3. Bacteria were grown at 37 °C in Luria Broth Lennox. 100 μg/ml Carbenicillin is added for selection of pUC18 and pGD93 derivatives, and 50 μg/ml spectinomycin for pBAD43 derivatives.

2.2. RNA preparation

Total RNAs were purified as previously described [5].

2.3. RNAseq experiments

RNAseq experiments were performed on RNA purified from *V. cholerae* N16961 grown at 37 °C in Luria Broth with 332 mM NaCl until exponential (OD_{600} = 0.4) and stationary growth phases. Directional libraries were prepared using the TruSeq Stranded mRNA Sample preparation kit following the manufacturer's instructions (Illumina). The libraries were quantified and sequenced as previously described [5]. Raw sequencing reads are treated, and count data analyzed as previously described [5]. The RNAseq data have been deposited in NCBI's Gene Expression Omnibus [23] and are accessible through GEO Series accession number GSE214813 (https://www.ncbi.nlm.nih.gov/geo/query/acc.cgi?acc=GSE214813).

2.4. Construction of TA systems expression vectors

Potential toxin genes were amplified from *V. cholerae* N16961 and subcloned into the expression vector pBAD43 under the control of the arabinose inducible promoter P_{ara}. Potential antitoxin genes were subcloned into the expression vector pUC18 under the control of the promoter P_{lac} as previously described [11]. All constructions were verified by sequencing. Primers are listed in Supplementary Table S4.

2.5. TA systems assays

TA systems assays were performed in DH5α *E. coli* strain, as previously described, in the presence of 1% glucose or 0.2% arabinose [12].

2.6. Two-hybrid assay

Two-Hybrid assay was performed using Bacterial Adenylate Cyclase Two-Hybrid System Kit (BACTH System Kit, Euromedex). VCA0497 was cloned in the low copy number plasmid pKT25 with N terminal fusion with T25 peptide (pP850) and VCA0498 the high copy number plasmid pUT18C with N terminal fusion with T18 peptide (pP852), both in *Pst*I and *Bam*HI sites. VCA0497-VCA0498 proteins interaction were visualized in BTH101 *E. coli* strain with blue coloration on LB Xgal IPTG kanamycin carbenicillin, following the manufacturer's instructions.

2.7. Measure of VCA0497-498 regulation with GFP-fusion assay

Fluorescence of $P_{VCA0497}$-GFP fusion (pN018) of overnight cultures of DH5α *E. coli* in LB, in the presence of antitoxin alone (pD918), of VCA0497-0498 entire operon (pN067) cloned in pUC18 or empty plasmid pUC18, was measured as previously described [24] using a Miltenyi MACSQuant flow cytometer. Experiments were performed with three independent cultures. A non-fluorescent *E. coli* strain culture (devoid of GFP) was used as negative control to calibrate the experiment and the proportion of fluorescent cells was measured at the FITC channel for tested samples carrying the GFP fusion. 100000 cells were counted for each sample.

2.8. SOS induction assay

SOS induction assay was performed, as previously described [25], using JJC610 strain (*E. coli* with *sfiA*:: *lacZ* fusion) in the presence of pBAD43 plasmid derivatives, after 3 h of growth at 37 °C in LB with 50 μg/ml spectinomycin, in triplicate.

2.9. RT-QPCR

RT-QPCR was adapted from [26]. For VCA0497 toxin, cultures of DH5α *E. coli* containing empty pBAD43 or with VCA0497 (pD611) were grown in M63 with 1% glucose, vitamin B1, spectinomycin 50 μg/ml, casamino acid 0.1% until OD_{600} reaches 0.2. Cultures were centrifuged, and pellet was diluted in same medium with 0.2% arabinose instead of glucose 1%, and let it grow 1 h. For VCA0495 toxin, cultures of DH5α *E. coli* containing pE652 and empty pBAD43 or with VCA0495** (pE879: pBAD43 expressing the toxin with both ncRNA495 and ncRNA496 inactivated promoters) were grown at 42 °C in LB with 1% glucose and spectinomycin 50 μg/ml, until OD_{600} reaches 0.4. Cultures were centrifuged, and pellet was

diluted at OD_{600} 0.05 in 42 °C preheated LB with spectinomycin 50 μg/ml, and let it grow one and 2 h at 42 °C.

Total RNAs were purified as previously described [5]. Reverse transcription was performed on 1 μg total RNA using primers 3' below with superscript III (Invitrogen) 50 min at 50 °C. Quantitative PCR was performed with Master Mix SYBR Green (Applied) using primers ompFQRT5bis and ompFGSP2-3, LppQPCR5 and LppQPCR3. Experiments was performed twice with independent cultures.

2.10. 5' RACE

5' RACE was performed on 1 μg total RNA with Smarter RACE 5'/3' (Takara) using primer ompFGSP2-3. cDNA fragments were amplified using primer ompfNgsp2 and UPM primer (Takara) with 40 cycles and visualized on agarose gel. They were subcloned in pTOPO plasmid using Zero blunt TOPO PCR cloning kit (Invitrogen). 48 clones were sequenced to identify the 5'-ends of the transcripts.

2.11. ncRNAs promoter directed mutagenesis

ncRNA488, ncRNA495 and ncRNA496 promoters were mutated using primers 309mut5 and 309mut3, 495mid5 and 495mid3, 495end5 and 495 end3, by complete amplification of wild type plasmid using Herculase II. After column purification, the amplification product was digested by DpnI to remove wild type plasmid and then transformed into DH5 α *E. coli*. Mutations were confirmed by sequencing. Plasmids are listed in Supplementary Table S1.

2.12. Construction of ncRNA495 thermosensitive expression vector

ncRNA495, with its own promoter, was subcloned inside high copy number heat-sensitive plasmid pGD93 [27] instead of *dam* gene using primers n495ecorI5 and n495pstI3, giving rise to pE652. The construction was verified by sequencing. Plasmid is listed in Supplementary Table S1.

2.13. VCA0495 toxicity assays in the presence of pE652

Various VCA0495 construction, under P_{ara} in pBAD43 in the presence of pE652 in DH5α *E. coli* strain, were grown in LB with carbenicillin and spectinomycin at 30 °C. Overnight cultures were diluted to 0.05 OD_{600} in the same conditions of growth or in LB with spectinomycin and arabinose 0.2% at 42 °C to induce VCA0495 gene expression and to eliminate pE652 thermosensitive plasmid. After 6 h, 5 μl of pure culture to $1/10^5$ were spotted on the same medium and incubating temperature than the liquid culture. Petri dishes were visualized after 24 h incubation.

2.14. tmRNA counteracting RelE toxicity assay

The two Gerdes and coll. Previously published protocols [28] were used after the following slight modifications to assay our toxins activity as RNase. For the first type of experiments, for VCA0497, MG1655ΔssrA strain [28] in the presence of pBR322 or pSC320 (*ssrA* and *smpB* in pBR322 [28]) and pBAD43 plasmid derivatives, were grown at 37 °C in M63 Vitamin B1 with 0.1% casamino acid, 0.04% arabinose, 0.4% succinate, 50 μg/ml spectinomycin, 15 μg/ml tetracycline. Precultures with 1% glucose were diluted at 0.05 OD_{600}. After 2 h, 10 μl of dilution were spotted on plates. After 24 h at 37 °C, spots were visualized. Experiment was performed twice. For VCA0495, precultures were performed at 30 °C in the presence of pE652 and carbenicillin and we used a pBR322 Δ*bla* instead of pBR322 wild-type. They were diluted at 0.1 OD_{600} in M63 Vitamin B1 with 0.1% casamino acid, 0.4% glycerol, 0.1% arabinose, 50 μg/ml spectinomycin, 15 μg/ml tetracycline at 42 °C. The curve

presented correspond to the medium of three independent cultures. For the second type of experiments, VCA0497 in pBAD43 (pD611) and VCA0498 in pSU18 (pR821) in MG1655 and MG1655ΔssrA strain [28] were grown at 37 °C in M63 Vitamin B1 with 0.1% casamino acid, 0.2% glucose, 50 μg/ml spectinomycin, 25 μg/ml chloramphenicol during 8 generations. At 0.4 OD_{600}, cultures were centrifuged and pellets were resuspended in M63 Vitamin B1 with 0.1% casamino acid, 0.5% glycerol, 0.1% arabinose, 50 μg/ml spectinomycin, 25 μg/ml chloramphenicol. At time 0, and after 15, 45 and 90 min of growth at 37 °C, cultures were spread on LB containing 0.2% glucose, 50 μg/ml spectinomycin, 25 μg/ml chloramphenicol and 0.5 mM IPTG. After 24 h at 37 °C, cfu were counted. Experiment was performed in triplicate.

2.15. RNase H assay

RNase H deficient *E. coli* strain MIC2067 is unable to grow at 42 °C in the absence of RNase H complementation [29]. This strain was transformed with pE652 and pE879 (VCA0495**). After 6 h of growth in LB spectinomycin, chloramphenicol, kanamycin and 0.2% arabinose at 42 °C, cultures were streaked on plate with same medium at 42 °C. Growth was visualized after 24 h.

3. Results

3.1. Identification of type II TA system candidates from RNAseq data analysis

In a previous study, we have established the whole transcriptome landscape, including coding and non-coding RNAs, as well as mapped their corresponding transcriptional start sites (TSS), of *V. cholerae* N16961 strain [5]. In this strain, we found that type II TA systems are organized as two-gene long operons, with a TSS positioned less than 37 bases upstream of the first gene ATG. When they are located in the SI, all these genetic elements are positioned within a single cassette. Since the majority of TA systems were previously found in the SI region, we first analyzed RNAseq data in this genome portion, looking for operons with uncharacterized function matching the description above. This led us to list of three eligible candidates: VCA0367-368, VCA0446-447, and VCA0497-498. Among these genes, only VCA0447 exhibited a predicted function: N6-methyltransferase. We then extended this analysis to whole genome and identified 6 additional operon candidates fulfilling the search criteria: VCA0208-209, located on the small chromosome, whose VCA0208 encoded a putative Nicotinate-nucleotide adenylyltransferase; VC0208-209, VC0333-334, VC0871-972, VC0849-850 and VC2470-2471, located on the large chromosome. VC0209 encoded a putative protein involved in stationary phase survival, VC0333 encoded a putative TetR family transcriptional regulator while VC0334 encoded a putative DHH phosphoesterase. VC0849-850 operon shows 56% of identity to RatA/RatB TA system domains, while VC2471 exhibits an antitoxin domain of the CptAB TA module (BlastP CDD domain).

To assay their potential toxin function, genes were subcloned in pBAD43 plasmid under the control of P_{ara} promoter (induced by arabinose and repressed by glucose), while for antitoxin activity assay, they were subcloned in the pUC18 plasmid under P_{lac} control. Toxicity of candidate genes and its counteraction by the partner genes were assayed in *E. coli* by using arabinose as the transcription inducer for the toxin, and IPTG for the antitoxin, as previously described [12]. Only the gene pair VCA0497-498 (Fig. 1A) led to a phenotype consistent with a TA system, unlike the other candidates (data not shown): upon arabinose induced expression (+Ara), VCA0497 alone kills *E. coli* (Fig. 1B), while co-expression of the
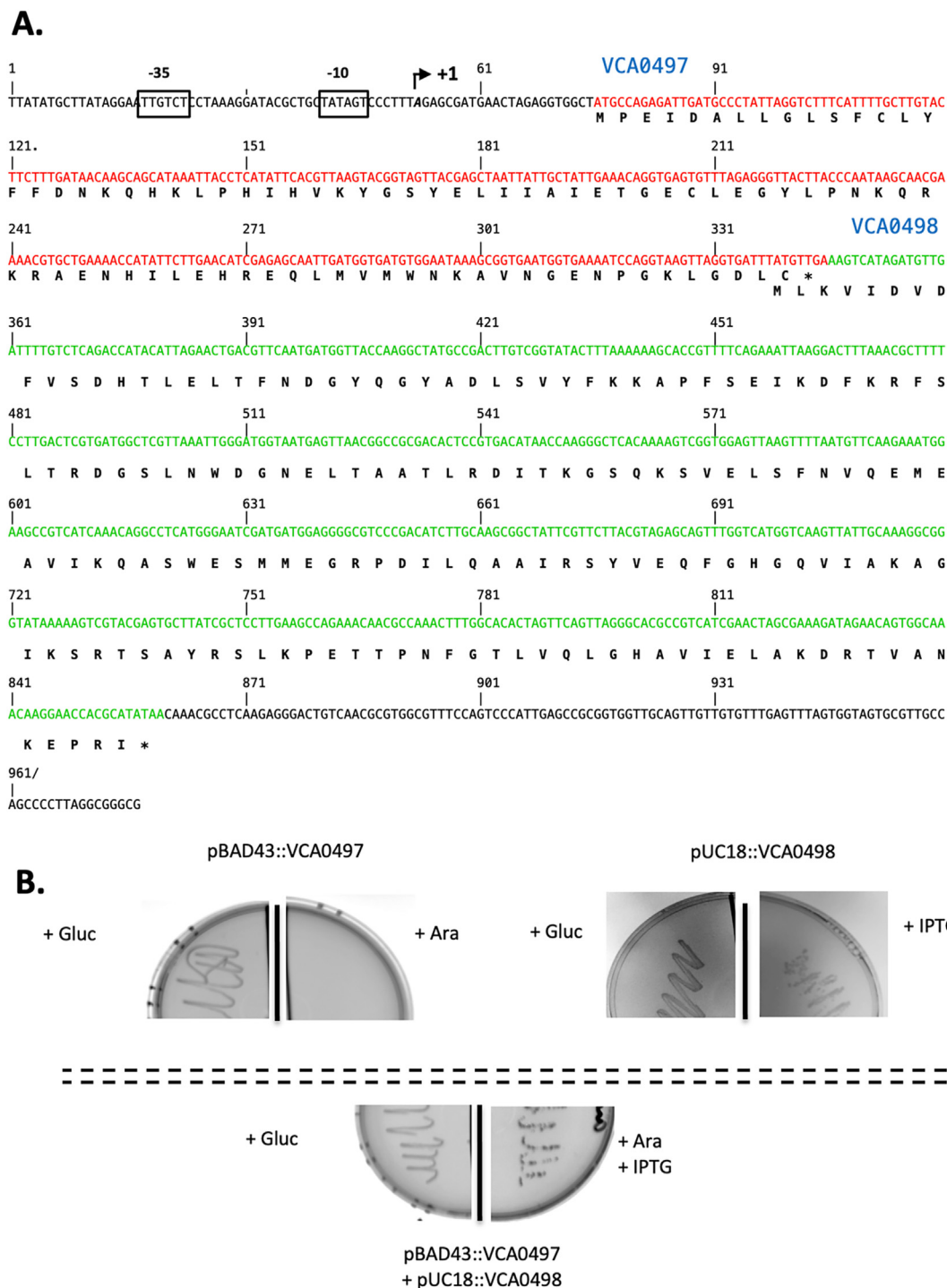
Fig. 1. New type II TA system VCA0497-0498 characterization. A. Sequence of the cassette carrying VCA0497-0498 operon, starting from the recombination point up to the end of the VCR and the next recombination point. The transcriptional start site (+1) is indicated by arrow and italic and bold letter. The −10 and −35 promoter sites are indicated with boxes. VCA0497, encoding the toxin, is shown in red letters, VCA0498 antitoxin in green letters. **B.** Plates showing growth of *E. coli* DH5α expressing VCA0497 from a P*ara* promoter in pBAD43, in the presence of glucose 1% (+Gluc) (repression) or arabinose 0.2% (+Ara) (high activation), VCA0498 from a P*lac* promoter into pUC18, in the presence of glucose 1% (repression) (+Gluc) or IPTG 0.8 mM (high activation) (+IPTG); or expressing both VCA0497 into pBAD43 and VCA0498 into pUC18, in the presence of glucose 1% (repression of both genes) (+Gluc) or arabinose 0.2% and IPTG 0.8 mM (high activation of both gene promoters) (+ Ara + IPTG). (For interpretation of the references to color in this figure legend, the reader is referred to the Web version of this article.)

associated VCA0498 in trans (+ Ara + IPTG) leads to bacterial survival (Fig. 1B).

Thus, among the nine candidates, the VCA0497-498 operon carried by a SI cassette is the only functional TA system associated with an antitoxin protein. The VCA0497-498 operon possesses a TSS located 17 bases upstream the VCA0497 start codon. It shows stable expression throughout exponential and stationary phase growth (RNAseq data), and is not induced by the SOS response [5].

3.2. Functional characterization of the VCA0498 antitoxin

We probed several protein structure databases with VCA0498 protein. This analysis revealed that the C-terminal part of the VCA0498 antitoxin matched with 3D structure of type II TA system antidote HipB, the antitoxin of the HipAB TA system, with 96.2% confidence in the Phyre 2 model [30]. HipB antitoxin acts by repressing the *hipAB* operon transcription, either alone or in protein complex with HipA, its cognate toxin [31,32]. Experiments were then performed to determine whether VCA0498 may similarly act as a repressor on its own operon promoter.

To characterize a potential interaction between VCA0497 and VCA0498 proteins, a bacterial two-hybrid experiment was performed. VCA0497 was cloned in the low copy number plasmid pKT25 with N terminal fusion with T25 peptide, while VCA0498 was cloned in the high copy number plasmid pUT18C with N terminal fusion with T18 peptide of the BACTH system kit and transformed in BTH101 reporter strain. The blue coloration obtained on LB Xgal IPTG kanamycin carbenicillin, corresponding to high activity of B-galactosidase reporter gene, was associated to interaction between the two proteins assayed. This suggested that VCA0498 antitoxin binds to its associated toxin (Fig. 2A).

To explore the impact of VCA0498 alone or associated with VCA0497 on their own operon promoter, we measured the effect of either the VCA0498 antitoxin expressed alone (pD918), or co-expressed with the VCA0497 toxin (pN067), on the transcription of a GFP reporter under the control of VCA0497-0498 operon promoter (pN018). VCA0498 antitoxin alone decreased 5.5-fold fluorescence level (p-value<0.01, student test), in comparison to the empty plasmid, while in the presence of both VCA0497 and VCA0498 fluorescence level was 16.2-fold decreased (p-value<0.01, student test) (Fig. 2B). This shows that the VCA0498 antitoxin functions similarly to HipB type II antitoxin, as it is able to repress the TA system operon transcription alone and also at a higher level with its partner toxin.

In conclusion, the VCA0497-VCA0498 operon encodes a new type II TA system, which shares the common properties of several type II TAs whose transcription is controlled by both the antitoxin alone and the toxin-antitoxin complex. This shows that the neutralization of the toxin occurs by both occlusion of its active site through the binding of the antitoxin and expression repression, as described for various type II TA systems [33–35].
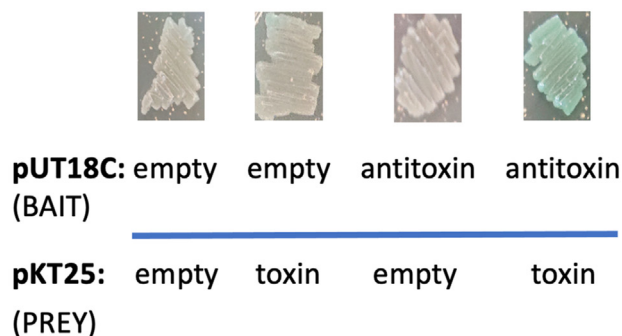
3.3. Functional characterization of the VCA0497 toxin

Despite using numerous domain and function prediction softwares, only a domain of unknown function, DUF4160, was identified in VCA0497 protein. We thus chose to explore known functions associated with characterized type II TA system toxins.

In order to test if this toxin acts on DNA, like the ParE family toxins which degrade DNA, leading to DNA damage that activates the SOS response [12,36,37], we investigated the effect of VCA0497 toxin on SOS response in *E. coli*. A *sfiA-lacZ* fusion (induced during SOS response [25]) was used to measure SOS response induction. A very low *sfiA-lacZ* increase was observed with VCA0497 toxin, in comparison to *parE1* (Table 1), suggesting the absence of DNA damage triggered by the VC0497 toxin. These results suggested that VCA0497 is not a DNAse.

A second category of toxins, such as e.g. RelE, HigB, or YhaV, proceeds by cleaving mRNAs [28,38,39] [40]. *lpp* and *ompF,* were previously used to assay mRNA degradation by RelE and YhaV toxin, respectively [28,40]. After 1 h of VCA0497 toxin induction on plasmid pBAD43, a little but not significant decrease (1.6-fold) was observed for *lpp* mRNA. On the other hand, we showed that VCA0497 toxin leads to a 72.1-fold decrease of the *ompF* mRNA
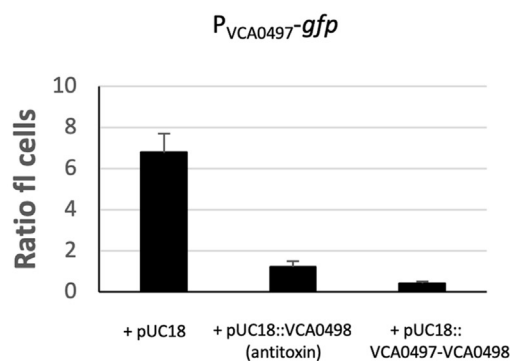

Fig. 2. Characterization of VCA0498 antitoxin. A. Two-Hybrid assay between VCA0497 and VCA0498, performed with BACTH System Kit. VCA0497 was cloned in pKT25 and VCA0498 in pUT18C. VCA0497-VCA0498 proteins interaction was visualized in *E. coli* BTH101 strain with blue coloration on LB Xgal IPTG kanamycin carbenicillin. **B**. Expression of GFP under VCA0497 promoter control (pN018). Green fluorescence was quantified in the absence (empty pUC18) and presence of VCA0498 antitoxin (pD918) and both VCA0498 antitoxin and VCA0497 toxin (pN067) in *E. coli*. Histogram bars represent the ratio of green fluorescence compared to the non-fluorescent strain and thus reflect transcription from the VCA0497 promoter. (For interpretation of the references to color in this figure legend, the reader is referred to the Web version of this article.)

Table 1
sfiA-lacZ induction by toxin. B-galacosidase was measured after 3 h toxin expression. Values corespond to mean values ± standard deviations of triplicate experiments.

Plasmids	Genotype	B-galacosidase (U/dry weight)
pBAD43	empty	1 ± 1
p7780	*parE1*	1030 ± 124
pD611	*VCA0497*	16 ± 1

level (pvalue<0.05, student test), in comparison to cells carrying an empty plasmid (QPCR and Fig. 3A). Sequencing analysis of *ompF* cDNAs obtained with 5' RACE experiment, revealed a hotspot cut 7 bases before the gene stop codon in the presence of VCA0497, while no similar cut was observed with the empty plasmid. This is compatible with the hypothesis of a specific endoribonuclease function associated to VCA0497 toxin, even in the absence of any identity to known ribonuclease catalytic domains.

As RelE, HigB, and YhaV toxins cleave mRNAs in a ribosome-dependent manner [41], we investigated the impact of over-expressing the tmRNA on the toxicity of VCA0497. Indeed, tmRNAs release stalled ribosomes from damaged mRNAs and rescues them,
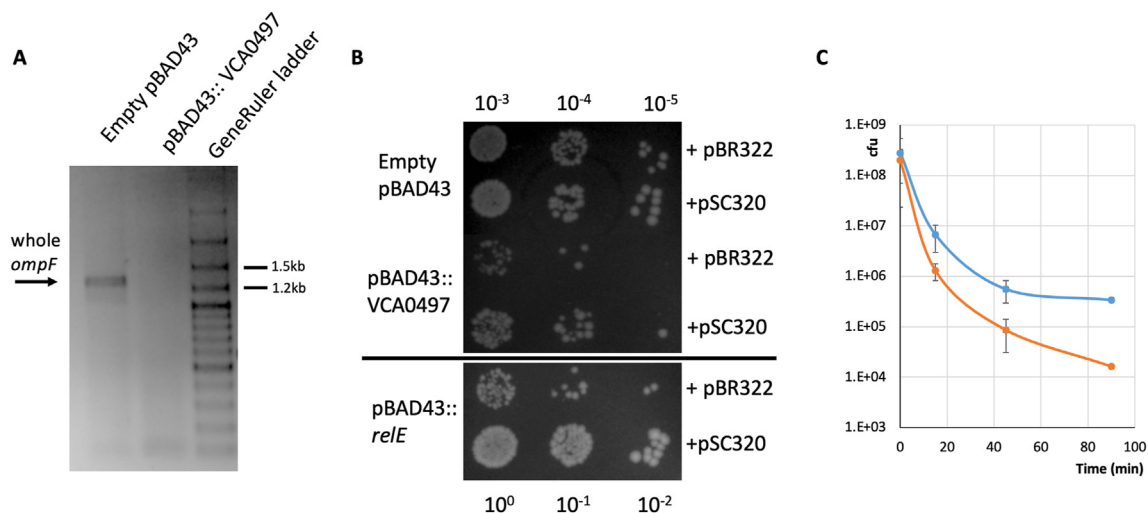
Fig. 3. VCA0497 toxin related ribonuclease function. A. *ompF* mRNA degradation: Agarose gel with whole *ompF* cDNA amplification after 5′RACE experiment from *E. coli* DH5α strain in the presence of VCA0497 or empty pBAD43 plasmid in *E. coli* DH5α strain, after 1 h arabinose induction. ***tmRNA* counteracted VCA0497 toxicity: B.** Spots of serial dilutions of cultures of *E. coli* MG1655Δ*ssrA* strain in the presence of *VCA0497* or *relE* cloned in pBAD43, or empty pBAD43 plasmid and pSC320 (*ssrA* and *smpB* in pBR322: *tmRNA* over-expression) or empty pBR322. **C.** After 0, 15, 45 and 90 min induction with 0.1% arabinose, cells containing both VCA0497 (pD611) and VCA0498 (pR821) in MG1655 or MG1655Δ*ssrA* (*tmRNA* deficient) strain were plated on LB with 0.2% glucose 0.5 mM IPTG spectinomycin and chloramphenicol, and CFU was counted. Blue curve: MG1655 strain; Red curve: MG1655Δ*ssrA* strain. (For interpretation of the references to color in this figure legend, the reader is referred to the Web version of this article.)

increasing survival in the presence of ribosome-dependent endoribonuclease family toxin [28]. We adapted the *in vivo* assay previously developed for RelE [28], based on the survival of a Δ*ssrA E. coli* strain containing a plasmid expressing the candidate toxin in the presence or absence of overexpressed tmRNA (*ssrA* and *smpB* cloned in pBR322 plasmid (pSC320)). After 2 h of growth, bacterial survival upon VCA0497 toxin expression is ten-fold higher in the presence of pSC320, in comparison to the empty pBR322, as observed in the control with the RelE toxin, while no difference was observed for empty pBAD43 (Fig. 3B). Thus, tmRNA increases the survival in the presence of VCA0497 toxin. To verify the role of tmRNA, we carried out a second experiment, also developed for RelE [28]. It compares survival between WT and *ssrA* (tmRNA) deficient MG1655 strains, in the presence of both toxin and anti-toxin, after toxin induction. We performed the assay with strains containing both VCA0497 toxin (pD611) and VCA0498 antitoxin (pR821). Survival in MG1655 was found to be always significantly higher (p value < 0.05, student test) than those observed in MG1655Δ*ssrA* strain (Fig. 3C). These results confirmed that tmRNA rescues mRNA cleavage triggered by the expression of the VCA0497 toxin. Again, this is compatible with a role of VCA0497, related to a ribosome-dependent endoribonuclease function.

3.4. VCA0497-VCA0498 encodes a dhiT/dhiA superfamily type II TA system

During our work, a new toxin also exhibiting a DUF4160 domain was recently identified in *Dickeya dadantii*, a plant pathogen bacteria, also found in fresh waters [42]. Protein comparison showed that VCA0497 has 64% identity with the newly identified DhiT toxin, while VCA0498 exhibits 59% homology with its associated DhiA antitoxin. This strongly suggests that VCA0497-VCA0498 encodes a *dhiT/dhiA* superfamily type II TA system. We thus called our genes *dhiT/dhiA* type II TA system.

3.5. The superintegron contains one type I TA system cassette

We next performed a second and different analysis of our RNAseq data from the SI region, looking for cassettes coding

potential type I TA system. Type I TA systems consist in general of a hydrophobic toxin protein, associated with antisense (AS) ncRNA, which plays the antitoxin role by interfering with the toxin mRNA stability and translation [21]. Based on these parameters, our analysis revealed that two cassettes were encoding a gene under its own promoter (with an identified TSS) and AS ncRNAs. These candidates corresponded to the cassettes carrying VCA0309, which encodes a putative endonuclease of 234 amino acids (aa), associated with AS ncRNA488; and VCA0495, which encodes a conserved hypothetical basic protein of 290 aa carrying hydrophobic domains (determined by Drawhca software), associated with two AS ncRNAs: ncRNA495 and ncRNA496 (Fig. 4A and Fig. 1 sup).

The toxicity of each gene was assayed in *E. coli* after cloning under the control of P_{ara} promoter and expression induction by arabinose, as described above. No growth defect, nor viability loss were observed when cells expressing either gene were incubated in the presence of arabinose, compared to growth in the presence of glucose. However, as the AS promoters are located inside the genes, the lack of toxicity could be related to a sufficiently high transcript level of AS ncRNAs to prevent protein toxicity, even when genes are overexpressed. To circumvent this possibility, the −10 box of each AS promoter was mutated, to abolish the AS ncRNA transcription, and thus its possible inhibitory effect on the toxin mRNA partner. The mutations introduced were synonymous changes, which thus kept unchanged the amino acid sequence of the toxin candidate. Mutation of the ncRNA488 promoter in VCA0309, did not affect *E. coli* cell viability when VCA0309 expression was induced by arabinose. We concluded that VCA0309 is likely not a toxin (or that it already carries inactivating mutations) and that the VCA0309-ncRNA488 couple, is not a type I TA system.

When this strategy was applied to VCA0495, we were unable to mutate simultaneously both ncRNA495 and ncRNA496 promoters, without getting other mutations likely impacting VCA0495 activity. This suggested that 1% of glucose didn't totally abolished P_{ara} dependent expression and that VCA0495 became toxic, in the absence of both AS ncRNAs. We then used a second approach, by adding in trans, ncRNA495 subcloned with its own promoter in the thermosensitive plasmid pGD93 [27], in *E. coli* recipient used for the toxicity assay. In this genetic context, we were able to mutate
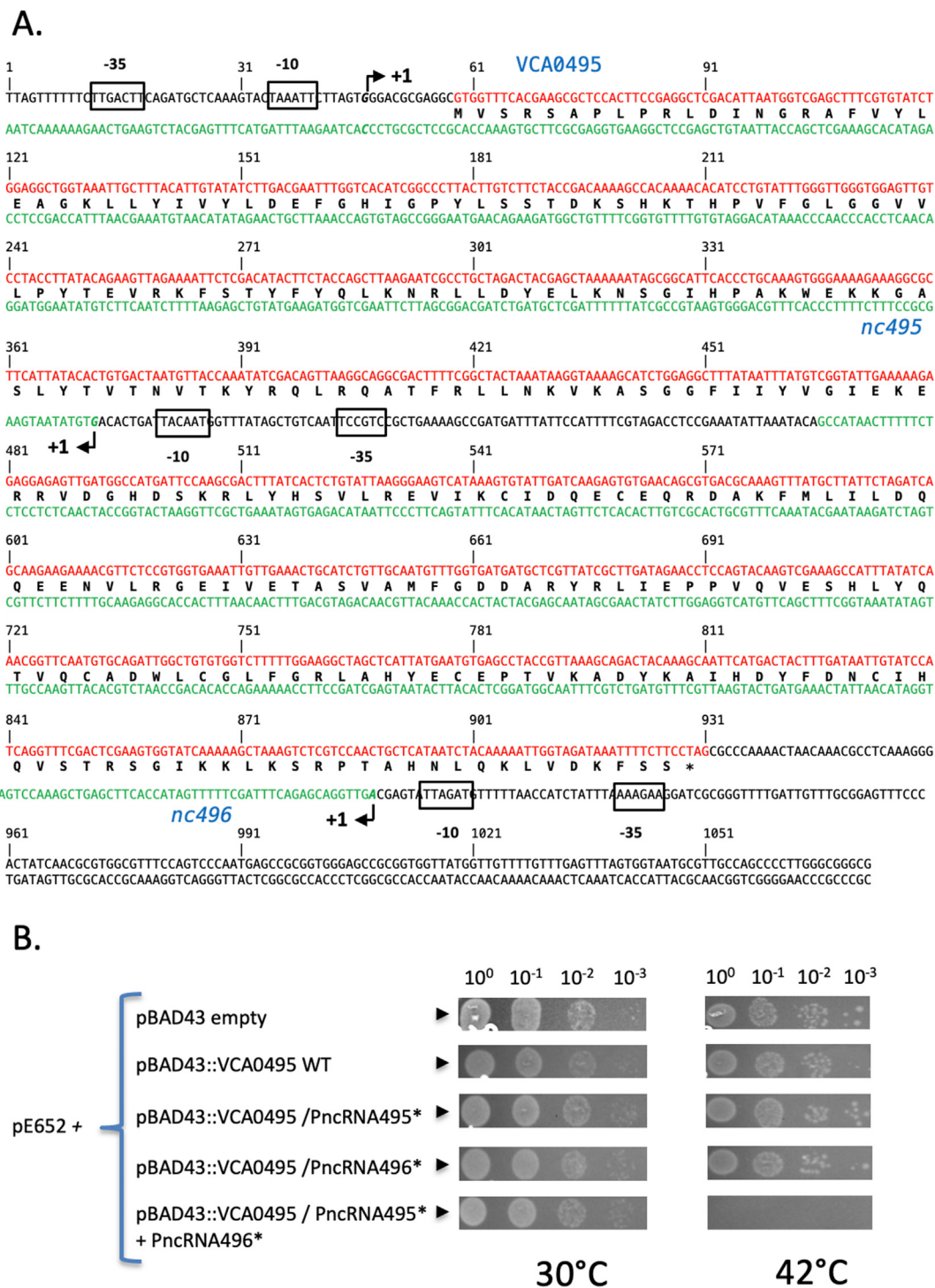
Fig. 4. Type I TA system VCA0495/ncRNA495 and ncRNA496 characterization. A. Sequence of the cassette carrying VCA0495 and its two ncRNAs, ncRNA495 and ncRNA496, starting from the recombination point up to the end of the VCR and the next recombination point. Gene nucleotidic sequence is red coloured, while non coding RNAs are green coloured. Transcriptional start sites (+1) are indicated by arrow and italic and bold letters. The −10 and −35 promoter sites are indicated with boxes. **B**. From top to bottom, spots of culture serial dilutions of *E. coli* DH5α carrying pE652 (ncRNA495 in thermosensitive PGD93) and either an empty pBAD43, a pBAD43 carrying the wild-type VCA0495 (pD612), or VCA0495 with ncRNA495 promoter mutated (*) (pI674), or VCA0495 with ncRNA496 promoter mutated (*) (pE348), or VCA0495 with both ncRNAs promoters mutated (*) (pE879), in the presence of spectinomycin and carbenicillin at 30 °C (left) or in the presence of spectinomycin and arabinose 0.2% at 42 °C (right). At 30 °C with carbenicillin, the ncRNA495 in trans is maintained and represses VCA0495 toxicity, by contrast, at 42 °C without carbenicillin and with arabinose, the ncRNA495 in trans is lost and VCA0495 is induced. (For interpretation of the references to color in this figure legend, the reader is referred to the Web version of this article.)

the ncRNA495 promoter in the plasmid harboring VCA0495 already carrying a mutated ncRNA496 promoter. In the *E. coli* host grown at 30 °C, when the plasmid expressing ncRNA495 in trans was

maintained, the survival was equivalent for all pBAD43 constructions (Fig. 4B). At 42 °C, when the plasmid expressing ncRNA495 in trans was lost, strains expressing the wild type toxin, or the two

synonymous versions with only one AS promoter inactivated, displayed an equivalent survival to those of control cells (with empty pBAD43) (Fig. 4B). By contrast, the strain carrying the plasmid expressing the toxin with both ncRNA495 and ncRNA496 mutated promoters (called VCA0495**), did not form colonies (Fig. 4B), demonstrating the toxicity of VCA0495.

Thus, this SI cassette encodes for a type I TA system, composed of VCA0495 toxin and two AS ncRNAs antitoxins (ncRNA495 and ncRNA496). This is the first report of such a type I TA in *V. cholerae*. VCA0495 toxin possesses a TSS located 12 bases upstream the gene start. Our transcriptomic data show that its expression level remained constant between exponential and stationary phase growth (RNAseq data) and that it was not regulated by SOS response [5].

3.6. Functional characterization of the VCA0495 toxin

As for the toxin above, we probed protein databases using several domain and function prediction softwares. We found the domain of unknown function DUF3800, as well as DNA and RNA binding domains (with Predict Protein) inside VCA0495 toxin. Moreover, it matched with 3D structure of ribonuclease H with 60.7% confidence, in the Phyre 2 modelization [30]. We then performed experiment to explore this function using the RNase H deficient *E. coli* strain MIC2067 [29]. No complementation phenotype was observed with VCA0495 toxin. However, the complementation was based on the MIC2067 ability to grow at 42 °C in the presence of RNase H gene; and the thermosensitive plasmid, that contained antitoxin ncRNA which represses VCA0495 toxin, was not lost from the beginning of 42 °C incubation. Thus, MIC2067 might die before VCA0495 was expressed. So, we can't absolutely exclude the possibility that this toxin is a ribonuclease.

Therefore, we explored RNase function, using the same *in vivo* experiment as for VCA0497 toxin on *lpp* and *ompF* targets (see above) with some adaptations, as the thermosensitive plasmid carrying AS ncRNA495 (pE652) was necessary to repress VCA0495** (see methods). To induce VCA0495** and eliminate pE652, growth monitoring was performed at 42 °C. After 1 h and 2 h of VCA0495 toxin expression, a slight increase (1.5 and 1.8-fold respectively), was observed for *lpp* mRNA level, while *ompF* mRNA level decreased 1.8 and 3.4-fold (pvalue<0.05, student test), respectively, in comparison to empty plasmid (QPCR and Fig. 5A). However, sequencing analysis of cDNAs didn't show any cleavage inside *ompF*.

To explore the tmRNA impact on VCA0495 toxicity, we also adapted protocol used for VCA0497, by monitoring the growth at 42 °C after arabinose induction. Data with RelE toxin are not shown, as bacterial growth stopped during lag phase. A growth slowdown was observed for cells expressing VCA0495** toxin in the presence of empty pBR322 after 5 h, leading to a growth arrest after 7 h (Fig. 5B); while growth continued in cells expressing VCA0495** toxin in the presence of the pSC320 (pBR322 overexpressing tmRNA), as well as in cells devoid of VCA0495 (empty pBAD43) associated to both pBR322 derivative plasmids (Fig. 5B). The pSC320/pBR322 growth ratio was significantly different between strains carrying VCA0495** toxin or empty pBAD43 ($p < 0,05$, student test) (Fig. 5B), showing that tmRNA rescues VCA0495 toxicity.

These results suggest that VCA0495 might have a ribonuclease activity.

4. Discussion

The multiplication of RNAseq experiments over the last 15 years has provided a wealth of data which can be exploited for the characterization of biological functions beyond transcription control studies only. Our work provides a new example of such approach, as we used the data, we previously generated, to establish the *V. cholerae* transcriptome, including TSS mapping [5], to identify possible uncharacterized toxin-antitoxin systems encoded in the genome of *V. cholerae* N16961. Based on the properties of characterized type II TA systems, we listed nine candidates two-genes operons, having a transcriptional start located close to the first gene initiation codon [5].

Toxicity assays led to the validation of a single type II TA system among these candidates, the VCA0497-0498 operon. It is located inside an integron cassette (Fig. 1), and carries its own promoter, with a TSS located 17 bases upstream of VCA0497 translation start. We found that antitoxin VCA0498, structurally related to the HipB antitoxin, acts as transcriptional repressor for the operon expression, alone, but also more strongly when in association with the toxin (Figs. 1 and 2). So, VCA0497 toxin neutralization occurs by both occlusion of its active site by the antitoxin and by expression decreases, as described in type II TA systems [33–35]. VCA0497 contains a DUF4160 domain, as the recently identified type II TA system DhiT toxin in *D. dadantii* [42] and has 64% identity with it. Moreover, VCA0498 exhibits 59% homology with its associated DhiA antitoxin. We thus called our genes *dhiT/dhiA* type II TA system. Our experiments suggest that VCA0497 DhiT toxin could be associated to a ribosome-dependent endoribonuclease function. Analysis of published *V. cholerae* transposon-insertion sequencing data [43] and unpublished experiment in LB at 37 °C from our laboratory revealed that both VCA0497 and VCA0498 are essential to bacterial survival. This is in agreement with the TA system functionality. Indeed, this confirms that in the absence of the antitoxin, or high TA system operon repression, the toxin is lethal. Moreover, the VCA0497-498 operon has stable expression throughout exponential and stationary phase growth like two other type II TA cassettes (VCA0468-469 and VCA0486-487) [11,12], while the majority of the TA cassettes are more expressed during exponential growth, when replication is active and thus cassette excision easier [44]. Genome data analysis shows that this TA system is found in two third of the fully or partially sequenced *V. cholerae* genomes (Table 1 sup). Proteins were identical in all, but one strains (NCTC 8457). In addition to *D. dadantii* [42], this TA family was also found (with at least 85% coverage and at least 50% identity) in several other marine bacteria: other *Vibrios, Halomonas, Shewanella, Nitrincola, Rheinheimera, Marinomonas, Photobacterium, Edwardsiella*. Acquisition through horizontal transfer among these marine species is thus likely at the origin of this large distribution. Moreover, in several *Vibrios (V. metoecus, V. fischeri, V. finisterrensis, V. sifiae)* and *Photobacterium (P. sanctipauli, P. leiognathi, P. phosphoreum)* species, these orthologous operons are located inside an integron cassette, as in *V. cholerae*.

In parallel, we performed a second analysis of the transcriptomic data from the superintegron region, looking for cassettes coding for potential type I TA system, *i.e.* cassette with a single gene and its promoter, and carrying AS ncRNA overlapping the coding region. Until now, no type I TA system had been described in *V. cholerae*. The genetic characterization we performed revealed that the *V. cholerae* SI possesses one type I TA system, composed of VCA0495 toxin and two embedded AS ncRNAs, ncRNA495 and 496. The toxin VCA0495, which carry a ribonuclease H domain may possibly possess a ribosome-dependent ribonuclease activity, however the experiment we performed did not reveal a specific cleavage pattern. Unlike several type I toxin genes [21], our previous study showed that VCA0495 transcription is not induced during SOS response [5]. However, as for the VCA0497-0498 type II TA system characterized above, its expression level remains constant between exponential and stationary phase growth.
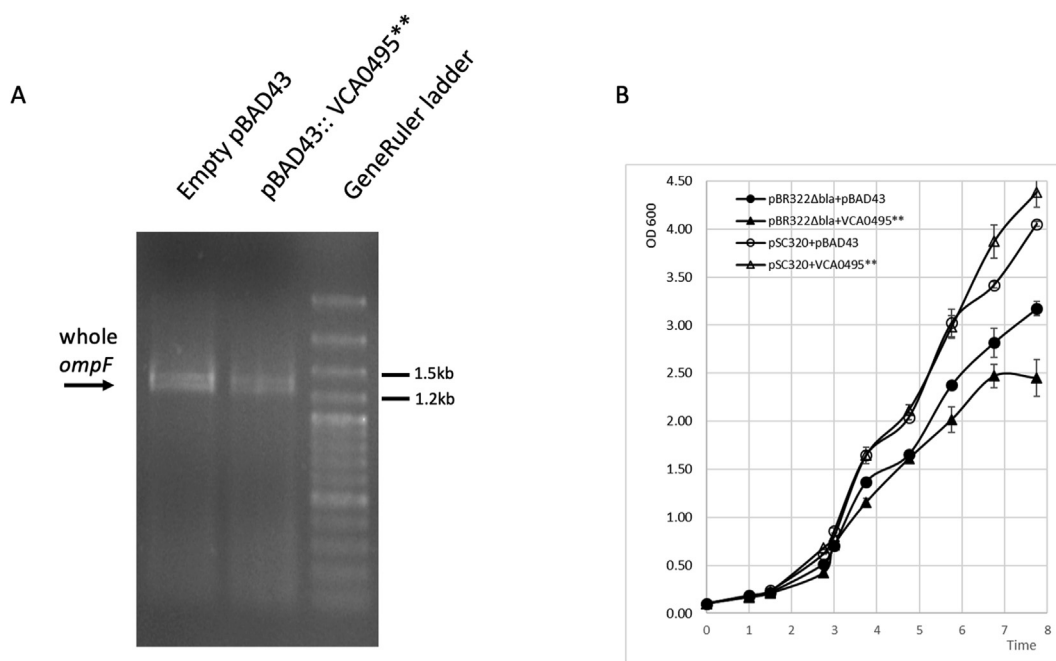
Fig. 5. Characterization of VCA0495 toxin. A. Agarose gel with whole *ompF* cDNA amplification after 5′RACE experiment from *E. coli* DH5α strain in the presence of VCA0495** (the synonymous toxin gene with both ncRNA495 and ncRNA496 mutated promoters) or empty pBAD43 plasmid in *E. coli* DH5α strain, after 2 h of expression. **B.** Growth of MG1655Δ*ssrA* strain in the presence of VCA0495** (cloned in pBAD43) or empty pBAD43 plasmid, and pBR322Δ*bla* or pSC320 (*ssrA* and *smpB* in pBR322) at 42 °C. As precultures with VCA0495 were performed at 30 °C in the presence of pE652 and carbenicillin, we used a pBR322 Δ*bla* instead pBR322 wild-type. pBR322Δ*bla* or pSC320 were maintained with tetracycline. This allowed pE652 lost during daytime growth, which is carbenicillin resistant.

It is puzzling that repression of VCA0495 necessitates the presence of two AS ncRNAs, especially as inactivation of the expression of either one or the other ncRNAs is not sufficient to reveal the VCA0495 toxicity, in standard growth conditions. A regulation by two AS ncRNAs is very rare. We found only one other example in the literature, for the transcriptional regulator CsgD. But in this case, both AS ncRNAs bind to the same *csgD* sequence region [45]. We hypothesize that a spontaneous mutation, leading to the creation of a second promoter, driving the synthesis of the second AS ncRNA, has increased the control of VCA0495 toxin expression and was maintained. Each AS ncRNA targets a different region of the toxin mRNA and therefore may have different effects. When the 5′ region of the mRNA is targeted, AS ncRNA might affect the transcription, while the second AS ncRNA might act on translatability. Moreover, it is, may be, very difficult to select a protein with an anti-VCA0495 activity, but the selection for an antitoxin activity from a ncRNA instead of a protein, may also be linked to the observed cassette size constraints. Indeed, the average size of sedentary chromosomal integron cassettes is below 700 bp, and while recombination of cassettes that are larger than 1.5 kb is possible, the one of 0.7 kb cassettes is approximately 10 times more efficient [46], likely imposing an important selective impediment on cassette coding capacity and TA system size. Another intriguing point is that all type I TA toxins characterized so far are small proteins (around 100 aa), be they targeting the membrane or acting as RNAse [47]. The size of the VCA0495 toxin, 290 aa, is thus unique and if we have no obvious explanation, we can only speculate that it has specific properties, which require a larger protein, perhaps for the recognition of its substrates or for its catalytic activity.

Genomic data analysis shows that this TA system is found in approximately two third of fully or partially sequenced *V. cholerae* genomes (With identical proteins in all but one strains 2740-80) and co-occurs with the type II TA system above, VCA0497-0498,

except in CT 5369-93 strain (Table S1). Comparison with other type II TA system shows only one another, VCA0477-0478 TA system which exhibits a similar distribution to the new type I TA system (except for TMA 21 strain).

The VCA0495 toxin orthologues show a much narrower distribution than the one of the VCA0497-0498 cassette described above. VCA0495 orthologues are found (with at least 85% coverage and at least 50% identity) in three other bacterial genomes (*Desulfurispirillum indicum* S5, *Gulbenkiania mobilis*, *Mesorhizobium* sp. WSM3873) and in the genome of the *Aeromonas* phage phiO18P. *Mesorhizobium* sp. WSM3873 was isolated on plants, while the other microorganisms have been found in environmental waters, i.e. sea or freshwater [48−50]. Furthermore, they are not carried in an integron cassette. A horizontal transfer may have occurred between environmental water microorganisms and *V. cholerae*.

Finally, when we look at the 19 TA cassettes distribution, considering these two new TA systems, one can see that their distribution along the SI cassette array is not homogenous. Indeed, there is clearly an enrichment in TA cassettes at the distal end of the SI, with 9 TA cassettes among the last 25 cassettes (which encompass ORFs VCA0468 up to VCA0506), while the first 10 TA cassettes are scattered among the previous 151 cassettes (Fig. 6). These TA systems are also found at the SI distal end, although in a different order, in *V. cholerae* strains M66, RC9, BX330286, V52 and CIRS101. Thus, if one cannot exclude that this local accumulation could be driven, at least partly, by an unknown property or role at this specific location, this uneven distribution likely reflects the cassette acquisition and loss dynamics. Cassettes' integration is favored at the *attI* sites in SIs [51] and thus new cassettes are selected at the *attI* proximal SI extremity, where they can be expressed. They are then pushed towards the distal end of the SI and silenced, after successive integrations of new cassettes, or reintegration of occasionally excised distal cassettes from the array,
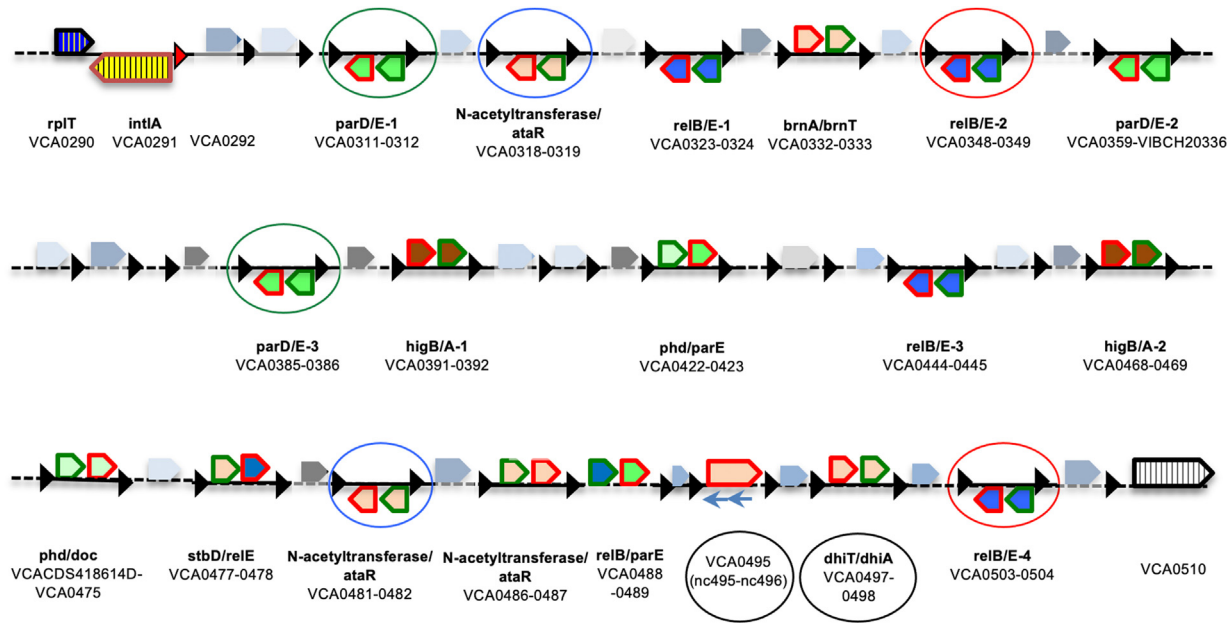
Fig. 6. Distribution of the toxin-antitoxin system cassettes in the *V. cholerae* N16961 superintegron. External boundaries of the SI cassette array are indicated by striped genes. Genes carried in cassettes are represented by plain pentagons, and attC sites (VCRs) are represented by triangles. TA genes are represented by pentagons framed in green for the antitoxins and in red for the toxins; the orientation of the pentagon and its location above or below the line indicate the orientation of the genes. Four defined toxin and antitoxin are indicated by the following colors: blue for *relB* and *relE*, green for *parD* and *parE*, brown for *higB* and *higA*, and light green for *phd* and *doc*. Identical TA cassettes are circled with same color. TA cassettes which have their names circled in black are those characterized in this study. Blue arrows correspond to non coding RNAs. (For interpretation of the references to color in this figure legend, the reader is referred to the Web version of this article.)

while TA system cassettes inserted among these, prevent deletion by slippage or illegitimate recombination events and locally stabilize the array [13,18]. However, these TA system cassettes which become detrimental when lost, cannot prevent single cassette loss through excision by the IntI integrase, especially as 73% of cassettes are promoterless [5] and thus silent when they are far from the SI *attI* site. Thus, one can expect that with time, the more distal a cassette is from the *attI* site, the higher is its chance to be lost, and that TA cassettes will accumulate at this SI end, as their loss will kill their host.

The identification of the two new TA systems, both located in the distal part of the SI cassette array, brings the total number of TA system cassettes in the *V. cholerae* N16961 SI up to 19. This clearly indicates that exploration of sedentary chromosomal integron cassette arrays, could unveil a wealth of new TA systems which can serve as a source for the stabilization of other mobile genetic elements.

Ethical statements

There are no ethical issues relevant to this work.

Declaration of competing interest

None.

Acknowledgements

Appendix A. Supplementary data

Supplementary data to this article can be found online at https://doi.org/10.1016/j.resmic.2022.103997.

References

[1] Heidelberg JF, Eisen JA, Nelson WC, Clayton RA, Gwinn ML, Dodson RJ, et al. DNA sequence of both chromosomes of the cholera pathogen *Vibrio cholerae*. Nature 2000;406:477—83.

[2] Mazel D, Dychinco B, Webb VA, Davies J. A distinctive class of integron in the *Vibrio cholerae* genome. Science 1998;280:605—8.

[3] Guerin E, Cambray G, Sanchez-Alberola N, Campoy S, Erill I, Da Re S, et al. The SOS response controls integron recombination. Science 2009;324:1034.

[4] Krin E, Cambray G, Mazel D. The superintegron integrase and the cassette promoters are co-regulated in *Vibrio cholerae*. PloS one 2014;9:e91194.

[5] Krin E, Pierle SA, Sismeiro O, Jagla B, Dillies MA, Varet H, et al. Expansion of the SOS regulon of Vibrio cholerae through extensive transcriptome analysis and experimental validation. BMC Genomics 2018;19:373.

[6] Barker A, Clark CA, Manning PA. Identification of VCR, a repeated sequence associated with a locus encoding a hemagglutinin in Vibrio cholerae O1. J Bacteriol 1994;176:5450—8.

[7] Ogawa A, Takeda T. The gene encoding the heat-stable enterotoxin of *Vibrio cholerae* is flanked by 123-base pair direct repeats. Microbiol Immunol 1993;37:607—16.

[8] Rowe-Magnus DA, Guerout AM, Mazel D. Bacterial resistance evolution by recruitment of super-integron gene cassettes. Mol Microbiol 2002;43:1657—69.

[9] Rowe-Magnus DA, Guerout AM, Ploncard P, Dychinco B, Davies J, Mazel D. The evolutionary history of chromosomal super-integrons provides an ancestry for multiresistant integrons. Proc Natl Acad Sci United State America 2001;98:652—7.

[10] Rowe-Magnus DA, Guerout AM, Biskri L, Bouige P, Mazel D. Comparative analysis of superintegrons: engineering extensive genetic diversity in the *Vibrionaceae*. Genome res 2003;13:428—42.

[11] Guerout AM, Iqbal N, Mine N, Ducos-Galand M, Van Melderen L, Mazel D. Characterization of the *phd-doc* and *ccd* toxin-antitoxin cassettes from *Vibrio* superintegrons. J Bacteriol 2013;195:2270−83.

[12] Iqbal N, Guerout AM, Krin E, Le Roux F, Mazel D. Comprehensive functional analysis of the eighteen *Vibrio cholerae* N16961 toxin-antitoxin systems substantiates their role in stabilizing the superintegron. J Bacteriol 2015;197: 2150−9.

[13] Szekeres S, Dauti M, Wilde C, Mazel D, Rowe-Magnus DA. Chromosomal toxin-antitoxin loci can diminish large-scale genome reductions in the absence of selection. Mol Microbiol 2007;63:1588−605.

[14] Wang X, Yao J, Sun YC, Wood TK. Type VII toxin/antitoxin classification system for antitoxins that enzymatically neutralize toxins. Trends Microbiol 2021;29: 388−93.

[15] Page R, Peti W. Toxin-antitoxin systems in bacterial growth arrest and persistence. Nat Chem Biol 2016;12:208−14.

[16] Blower TR, Short FL, Rao F, Mizuguchi K, Pei XY, Fineran PC, et al. Identification and classification of bacterial Type III toxin-antitoxin systems encoded in chromosomal and plasmid genomes. Nucleic Acids Res 2012;40:6158−73.

[17] Pandey DP, Gerdes K. Toxin-antitoxin loci are highly abundant in free-living but lost from host-associated prokaryotes. Nucleic acids res 2005;33: 966−76.

[18] Hayes F. Toxins-antitoxins: plasmid maintenance, programmed cell death, and cell cycle arrest. Science 2003;301:1496−9.

[19] Goeders N, Van Melderen L. Toxin-antitoxin systems as multilevel interaction systems. Toxins 2014;6:304−24.

[20] Fozo EM, Hemm MR, Storz G. Small toxic proteins and the antisense RNAs that repress them. Microbiol mol biol rev : MMBR (Microbiol Mol Biol Rev) 2008;72:579−89.

[21] Gerdes K, Wagner EG. RNA antitoxins. Curr Opin Microbiol 2007;10:117−24.

[22] Fozo EM, Makarova KS, Shabalina SA, Yutin N, Koonin EV, Storz G. Abundance of type I toxin-antitoxin systems in bacteria: searches for new candidates and discovery of novel families. Nucleic Acids Res 2010;38:3743−59.

[23] Edgar R, Domrachev M, Lash AE. Gene Expression Omnibus: NCBI gene expression and hybridization array data repository. Nucleic Acids Res 2002;30:207−10.

[24] Baharoglu Z, Bikard D, Mazel D. Conjugative DNA transfer induces the bacterial SOS response and promotes antibiotic resistance development through integron activation. PLoS Genet 2010;6:e1001165.

[25] Flores MJ, Sanchez N, Michel B. A fork-clearing role for UvrD. Mol Microbiol 2005;57:1664−75.

[26] Culviner PH, Nocedal I, Fortune SM, Laub MT. Global analysis of the specificities and targets of endoribonucleases from *Escherichia coli* toxin-antitoxin systems. mBio 2021;12:e0201221.

[27] Demarre G, Chattoraj DK. DNA adenine methylation is required to replicate both *Vibrio cholerae* chromosomes once per cell cycle. PLoS Genet 2010;6: e1000939.

[28] Christensen SK, Gerdes K. RelE toxins from bacteria and Archaea cleave mRNAs on translating ribosomes, which are rescued by tmRNA. Mol Microbiol 2003;48:1389−400.

[29] Itaya M, Omori A, Kanaya S, Crouch RJ, Tanaka T, Kondo K. Isolation of RNase H genes that are essential for growth of *Bacillus subtilis* 168. J Bacteriol 1999;181:2118−23.

[30] Kelley LA, Mezulis S, Yates CM, Wass MN, Sternberg MJ. The Phyre2 web portal for protein modeling, prediction and analysis. Nat Protoc 2015;10: 845−58.

[31] Wen Y, Behiels E, Felix J, Elegheert J, Vergauwen B, Devreese B, et al. The bacterial antitoxin HipB establishes a ternary complex with operator DNA and phosphorylated toxin HipA to regulate bacterial persistence. Nucleic Acids Res 2014;42:10134−47.

[32] Schumacher MA, Piro KM, Xu W, Hansen S, Lewis K, Brennan RG. Molecular mechanisms of HipA-mediated multidrug tolerance and its neutralization by HipB. Science 2009;323:396−401.

[33] Kamada K, Hanaoka F. Conformational change in the catalytic site of the ribonuclease YoeB toxin by YefM antitoxin. Mol Cell 2005;19:497−509.

[34] Kamada K, Hanaoka F, Burley SK. Crystal structure of the MazE/MazF complex: molecular bases of antidote-toxin recognition. Mol Cell 2003;11:875−84.

[35] Miallau L, Faller M, Chiang J, Arbing M, Guo F, Cascio D, et al. Structure and proposed activity of a member of the VapBC family of toxin-antitoxin systems. VapBC-5 from *Mycobacterium tuberculosis*. J Biol Chem 2009;284:276−83.

[36] Yuan J, Sterckx Y, Mitchenall LA, Maxwell A, Loris R, Waldor MK. Vibrio cholerae ParE2 poisons DNA gyrase via a mechanism distinct from other gyrase inhibitors. J Biol Chem 2010;285:40397−408.

[37] Yuan J, Yamaichi Y, Waldor MK. The three *Vibrio cholerae* chromosome II-encoded ParE toxins degrade chromosome I following loss of chromosome II. J Bacteriol 2011;193:611−9.

[38] Budde PP, Davis BM, Yuan J, Waldor MK. Characterization of a higBA toxin-antitoxin locus in Vibrio cholerae. J Bacteriol 2007;189:491−500.

[39] Christensen-Dalsgaard M, Gerdes K. Two *higBA* loci in the *Vibrio cholerae* superintegron encode mRNA cleaving enzymes and can stabilize plasmids. Mol Microbiol 2006;62:397−411.

[40] Choi W, Yamaguchi Y, Lee JW, Jang KM, Inouye M, Kim SG, et al. Translation-dependent mRNA cleavage by YhaV in *Escherichia coli*. FEBS Lett 2017;591: 1853−61.

[41] Han Y, Lee EJ. Substrate specificity of bacterial endoribonuclease toxins. BMB Rep 2020;53:611−21.

[42] Boss L, Gorniak M, Lewanczyk A, Morcinek-Orlowska J, Baranska S, Szalewska-Palasz A. Identification of three type II toxin-antitoxin systems in model bacterial plant pathogen *Dickeya dadantii* 3937. Int J Mol Sci 2021;22.

[43] Chao MC, Pritchard JR, Zhang YJ, Rubin EJ, Livny J, Davis BM, et al. High-resolution definition of the *Vibrio cholerae* essential gene set with hidden Markov model-based analyses of transposon-insertion sequencing data. Nucleic Acids Res 2013;41:9033−48.

[44] Loot C, Bikard D, Rachlin A, Mazel D. Cellular pathways controlling integron cassette site folding. EMBO J 2010;29:2623−34.

[45] Holmqvist E, Reimegard J, Sterk M, Grantcharova N, Romling U, Wagner EG. Two antisense RNAs target the transcriptional regulator CsgD to inhibit curli synthesis. EMBO J 2010;29:1840−50.

[46] Loot C, Nivina A, Cury J, Escudero JA, Ducos-Galand M, Bikard D, et al. Differences in integron cassette excision dynamics shape a trade-off between evolvability and genetic capacitance. mBio 2017;8:22966. e2316.

[47] Brantl S, Jahn N. sRNAs in bacterial type I and type III toxin-antitoxin systems. FEMS Microbiol Rev 2015;39:413−27.

[48] Beilstein F, Dreiseikelmann B. Temperate bacteriophage *PhiO18P* from an *Aeromonas* media isolate: characterization and complete genome sequence. Virology 2008;373:25−9.

[49] Rauschenbach I, Narasingarao P, Haggblom MM. *Desulfurispirillum indicum* sp. nov., a selenate- and selenite-respiring bacterium isolated from an estuarine canal. Int J Syst Evol Microbiol 2011;61:654−8.

[50] Vaz-Moreira I, Nobre MF, Nunes OC, Manaia CM. *Gulbenkiania mobilis* gen. nov., sp. nov., isolated from treated municipal wastewater. Int J Syst Evol Microbiol 2007;57:1108−12.

[51] Vit C, Richard E, Fournes F, Whiteway C, Eyer X, Lapaillerie D, et al. Cassette recruitment in the chromosomal Integron of Vibrio cholerae. Nucleic Acids Res 2021;49:5654−70.